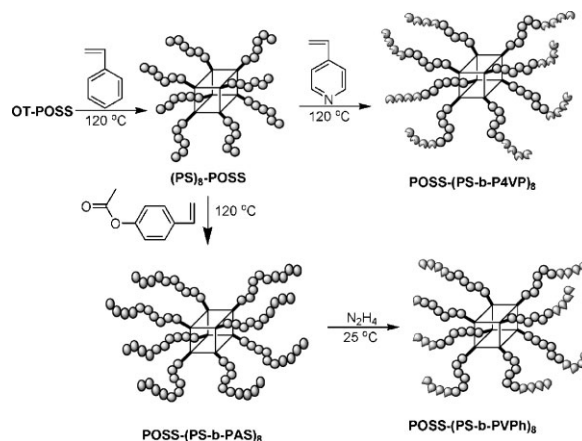


# Star Block Copolymers Through Nitroxide-Mediated Radical Polymerization From Polyhedral Oligomeric Silsesquioxane (POSS) Core

Chu-Hua Lu, Jui-Hsu Wang, Feng-Chih Chang, Shiao-Wei Kuo\*

A series of star block copolymers were prepared through nitroxide-mediated radical polymerization (NMRP) from polyhedral oligomeric silsesquioxanes (POSS) nanoparticle by core-first polymerization. Eight *N*-alkoxyamine groups were incorporated onto the eight corners of a POSS cube through quantitative hydrosilylation through addition of octakis(dimethylsiloxy)silsesquioxane ( $Q_8M_8^H$  POSS) with 1-(2-(allyloxy)-1-phenylethoxy)-2,2,6,6-tetramethylpiperidine (allyl-TEMPO) and Karstedt's agent (a platinum divinylsiloxane complex) was used as a catalyst. Octa-*N*-alkoxyamines POSS (OT-POSS) were used as platform to synthesize star polystyrene-POSS ((PS)<sub>8</sub>-POSS) homopolymer and diblock copolymers of poly(styrene-*block*-4-vinylpyridine)-POSS ((PS-*b*-P4VP)<sub>8</sub>-POSS) and poly(styrene-*block*-acetoxystyrene) ((PS-*b*-PAS)<sub>8</sub>-POSS) through NMRP. In addition, subsequent selective hydrolysis of the acetyl protective group of (PS-*b*-PAS)<sub>8</sub>-POSS, the poly(styrene-*block*-vinyl phenol) ((PS-*b*-PVPh)<sub>8</sub>-POSS) with strong hydrogen bonding group was obtained. The detailed chemical structure and self-assembled structures of these star block copolymers based on POSS were characterized by <sup>1</sup>H NMR, FTIR, SEC, TEM, and SAXS analyses.



## Introduction

Star polymers are macromolecules consisting of more than three linear polymer chains of approximately equal lengths joined together at one end of each chain to a chemically bonded core. The synthesis and characterization of star polymers continue to be areas of exploration in the pursuit of structure–property relationships in macromolecular science.<sup>[1]</sup> Star polymers have attracted great interest, especially from the viewpoints of their rheological and

C.-H. Lu, J.-H. Wang, F.-C. Chang  
Institute of Applied Chemistry, National Chiao Tung University,  
Hsin Chu 300, Taiwan  
S.-W. Kuo  
Department of Materials and Optoelectronic Science, Center for  
Nanoscience and Nanotechnology, National Sun Yat-Sen  
University, Kaohsiung 804, Taiwan  
Fax: (+886) 7 5254099; E-mail: kuosw@faculty.nsysu.edu.tw

physical properties and their potential applications.<sup>[2,3]</sup> Methods for making star polymers fall into two broad classes. In the “arm first” approach, monofunctional living linear macromolecules are synthesized initially. Star formation then occurs in one of two ways: a difunctional comonomer is used to provide cross-linking through propagation<sup>[4,5]</sup> or a multifunctional terminating agent is added connecting a precise number of arms to a central core molecule. The second method for synthesizing star polymers is the “core-first” approach. Multifunctional initiators are used to grow chains from a central core resulting in macromolecules with well-defined structures in terms of both the number and length of the arms.<sup>[6–9]</sup> Furthermore, the reaction product consists solely of star polymers — there is an absence of linear polymers. In many cases, however, the multifunctional initiators must be presynthesized and, in addition, only a limited number of studies have used this method because of the poor solubility of the multiply charged species needed to initiate ionic polymerizations.<sup>[10–16]</sup>

Polyhedral oligomeric silsesquioxane (POSS) derivatives comprise a family of molecularly precise, near-isotropic molecules that have diameters ranging from 1 to 3 nm, depending on the number of silicon atoms in the central cage and the nature of its peripheral substituent groups.<sup>[17–23]</sup> A cubic  $T_8$  silsesquioxane unit possesses a cubic inorganic  $Si_8O_{12}$  core surrounded by eight tunable substituent groups. POSS has been recognized as a well-defined building block for nanostructured materials.<sup>[24–28]</sup> The cubic silsesquioxane unit can not only be viewed as a nanoparticle for both its size and filler function, but also a well-defined macromonomer for its ability to undergo polymerization. It appears logically that two well-defined macromolecular architectures, POSS, and star polymers, could be combined to generate polymer building blocks with well-defined 3D shapes, which dictate the self-assembly process and resulting in supramolecular structures. Because of their unique structures, POSS derivatives are useful building blocks for the preparation of nanostructured materials.<sup>[29,30]</sup>

Many of them have been prepared by using POSS initiators or monomers; however, few reports have utilized the living and controlled radical polymerization (LCRP) from an eight-functional POSS initiator.<sup>[31,32]</sup> Applying POSS monomers or initiators to LCRP is desirable to develop novel materials of varying composition, topology, and well-defined molecular weights. The synthesis of star homopolymers or block copolymers using the cubic POSS as a nanosized multifunctional initiator is particularly interesting. In this work, we report the nitroxide-mediated radical polymerization (NMRP) of styrene, 4-vinylpyridine, and 4-acetoxystyrene monomers. Using this approach we have synthesized star homopolymers and block copolymers from an octa-*N*-alkoxyamine-functionalized POSS core (OT-

POSS). Considering that the eight *N*-alkoxyamine unimolecular initiators of NMRP are located on the eight corners of a POSS cube (OT-POSS), the propagation of NMRP extending from such a bulk POSS cube is feasible and promising for an LCRP of well-defined architectures. Here, the polymerization of a star homopolymer [(PS)<sub>8</sub>-POSS] and star block copolymers of [poly(styrene-*block*-4-vinylpyridine)-POSS ((PS-*b*-P4VP)<sub>8</sub>-POSS) and poly(styrene-*block*-acetoxystyrene) ((PS-*b*-PAS)<sub>8</sub>-POSS)] can demonstrate the quantitative hydrosilylation to produce OT-POSS and the well-controlled NMRP (narrow distribution of molecular weights) from OT-POSS. The detailed chemical structure, thermal property, and self-assembly structure of these star block copolymers based on POSS were characterized by <sup>1</sup>H NMR, FTIR, SEC, DSC, TEM, and SAXS analyses.

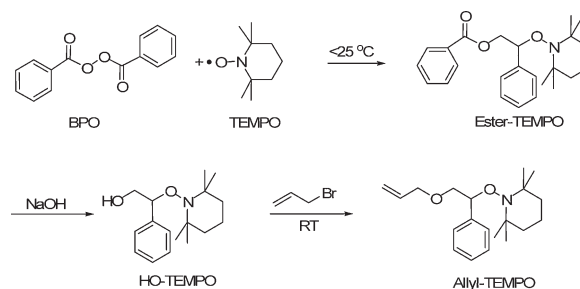
## Experimental Part

### Materials

Octakis(dimethylsiloxy)silsesquioxane ( $O_8M_8^H$  POSS) was obtained from Hybrid Plastics. 4-Vinylpyridine, 4-acetoxystyrene (96%), styrene, hydrazine monohydrate (98%), and platinum (0)/1,3-divinyl-1,1,3,3-tetramethylidisiloxane complex solution [Pt(dvs)] in xylene (Pt content = ca. 2%), were obtained from Aldrich Chemical (USA). The following chemicals and solvents were used as-received: benzoyl peroxide (BPO, >97%, Fluka), styrene (St, 99%, ACROS), 2,2,6,6-tetramethylpiperidinoxy (TEMPO, 98%, ACROS), tetrahydrofuran (THF, HPLC grade, TEDIA), methanol (MeOH, HPLC grade, TEDIA), and diethyl ether (Et<sub>2</sub>O, HPLC grade, TEDIA). Reactions were performed in glassware under a static atmosphere of argon.

### The Synthesis of 1-(2-(Allyloxy)-1-phenylethoxy)-2,2,6,6-tetramethylpiperidine

The synthesis of 1-(2-(allyloxy)-1-phenylethoxy)-2,2,6,6-tetramethylpiperidine (allyl-TEMPO) was shown in Scheme 1. 5 *N*-alkoxyamine adduct HO-TEMPO<sup>[33–36]</sup> (3.42 mL in anhydrous THF, 17.1 mmol) was added dropwise to an anhydrous THF solution of 10 *N* potassium hydride KH (8.56 mL, 85.6 mmol, washed by hexane extraction). After stirring for 1 h, the upper clear solution was transferred to a new round bottle and 5 *N* allyl bromide (4.14 mL in anhydrous THF, 34.2 mmol) was added dropwise. For another 24 h,



■ Scheme 1. Preparation of allyl-TEMPO.

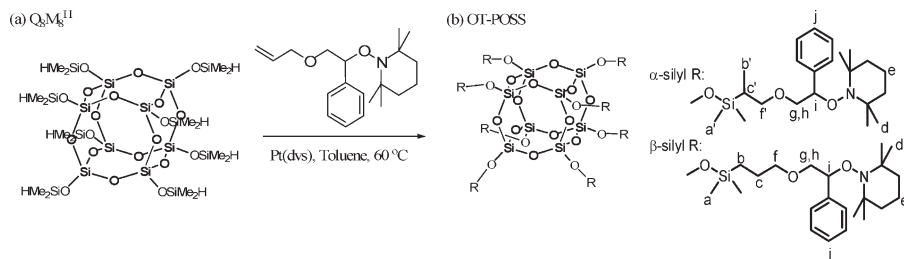
the product was purified by column chromatography. After rotary evaporation, allyl-TEMPO (4.5 g, 83%) was obtained as a light-yellow liquid. Mass spectra (ESI,  $m/z$ ): 318 [ $MH^+$ ]; Elem. Anal. for  $C_{20}H_{31}NO_2$ : Calcd. C 75.67, H 9.84, N 4.41; Found C 75.45, H 8.99, N 4.43.  $^1H$  NMR ( $CDCl_3$ )  $\delta$  0.64, 1.03, 1.19, 1.35 (each br s, 12H,  $CH_3$ ), 1.38–1.72 (m, 6H,  $CH_2$ ); 3.65 (ABq,  $J=10$  Hz, 6.5H,  $CHH$ ), 3.90 (m, 2H,  $CH_2$ ), 3.96 (ABq,  $J=10$  and 5 Hz, 1H,  $CHH$ ), 4.83 (ABq,  $J=6.5$  and 5 Hz, 1H,  $CH$ ), 5.12 (m, 1H,  $CH$ ), 5.79 (m,  $CH_2$ ), and 7.25–7.56 (m, 5H,  $ArH$ );  $^{13}C$  NMR ( $CDCl_3$ )  $\delta$  17.16, 20.34, 40.49, 72.05, 72.88, 85.37, 116.39, 127.22, 127.79, 127.83, 134.89, and 141.95.

### The Synthesis of OT-POSS

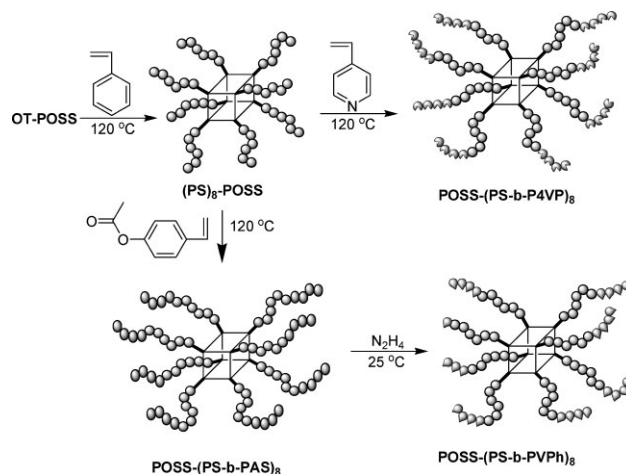
The synthesis of an OT-POSS initiator is the first step in the preparation of well-defined hybrid polymers using hydrosilylation as shown in Scheme 2. In a 100-mL Schlenk flask equipped with a reflux condenser and a magnetic stirrer, a solution of  $Q_8M_8^{II}$  (2.95 mmol) and allyl-TEMPO (23.57 mmol) in toluene (30 mL) was heated at 50 °C under argon and then Pt(dvs) (0.2 mL, 0.4  $\mu$ mol) was added via syringe. The reaction, which was monitored by measuring the decrease in intensity of the FTIR spectral signal at 2 134  $cm^{-1}$  for the Si–H bonds, was completed after 4 h.

### The Synthesis of Star (PS-*b*-P4VP)<sub>8</sub>-POSS, (PS-*b*-PAS)<sub>8</sub>-POSS, and (PS-*b*-PVPh)<sub>8</sub>-POSS Diblock Copolymers

The synthesis of star polystyrene [(PS)<sub>8</sub>-POSS] from OT-POSS is the second step in the preparation of well-defined hybrid polymers using NMRP (Scheme 3). In the NMRP of styrene, heating the mixture of OT-POSS ( $11.4 \times 10^{-3}$  M for target  $\bar{M}_n = 80\,000$  g · mol<sup>-1</sup>) and styrene at 120 °C gives monomer conversion at 80% after 17 h. In the NMRP of 4-vinylpyridine or 4-acetoxystyrene, the residual styrene in the (PS)<sub>8</sub>-POSS was removed by vacuum distillation at 25 °C and followed by adding 3-fold weights of 4-vinylpyridine or 4-acetoxystyrene to dissolve (PS)<sub>8</sub>-POSS and heated at 120 °C for 3 h. Analyses of the purified (PS-*b*-P4VP)<sub>8</sub>-POSS and (PS-*b*-PAS)<sub>8</sub>-POSS by  $^1H$  NMR revealed that the repeating units of P4VP and PAS per arm reached 20 (about 2 100 g · mol<sup>-1</sup>) and 24 (about 3 890 g · mol<sup>-1</sup>) by comparing protons from the styryl, pyridyl, and methyl protons. The synthesis of poly(styrene-*block*-vinyl phenol) ((PS-*b*-PVPh)<sub>8</sub>-POSS) was prepared by selectively acetoxy hydrazinolysis of (PS-*b*-PAS)<sub>8</sub>-POSS with hydrazine monohydrate.<sup>[37–41]</sup> Hydrazine monohydrate (1.73 g, 34.6 mmol, 16.0 equiv.) was added to a solution of (PS-*b*-PAS)-POSS (5.00 g, 2.16 mmol) in 1,4-dioxane. The acetoxy hydrazinolysis, which was monitored by measuring the



Scheme 2. Preparation of OT-POSS.



Scheme 3. Synthesis of (PS)<sub>8</sub>-POSS, (PS-*b*-P4VP)<sub>8</sub>-POSS, (PS-*b*-PAS)<sub>8</sub>-POSS, and (PS-*b*-PVPh)<sub>8</sub>-POSS.

decrease in intensity of the FTIR spectral signal for the C=O bond at 1 762  $cm^{-1}$ , was complete after 2 h.

### Characterizations

Using  $CDCl_3$  as the solvent,  $^1H$  NMR spectra were recorded on a Varian Unity Inova 500 FT NMR spectrometer operated at 500 MHz; chemical shifts are reported in parts per million (ppm). Molecular weight and molecular weight distribution were determined through gel permeation chromatography (GPC) using a Waters 510 HPLC equipped with a 410 differential refractometer, a refractive index (RI) detector, and three Ultrastaygel columns (100, 500, and 10<sup>3</sup>) connected in series for increasing pore size (eluent: DMF-*d*<sub>7</sub>, flow rate: 0.6 mL · min<sup>-1</sup>). FTIR spectrum of the KBr disk was measured using a Nicolet Avatar 320 FTIR Spectrometer, 32 scans were collected at a resolution of 1  $cm^{-1}$ . The sample chamber was purged with nitrogen to maintain film dryness. Thermal analysis was carried out using a DSC instrument (TA Instruments Q-20). The sample (ca. 4–6 mg) was weighed and sealed in an aluminum pan. The glass transition temperature ( $T_g$ ) was taken as the midpoint of the heat capacity transition between the upper and lower points of deviation from the extrapolated glass and liquid lines with a scan rate of 20 °C · min<sup>-1</sup> and a temperature range of 25–200 °C. Transmission electron microscopic (TEM) analysis was performed using a Hitachi H-7100 electron micro-

scope operated at 100 kV. Ultrathin sections of the samples were prepared using a Leica Ultracut S microtome equipped with a diamond knife. The ultrathin sections were picked onto the copper grids coated with carbon-supporting films followed by staining by exposure to the vapor of 4%  $RuO_4$  aqueous solution for 25 min. Small-angle X-ray scattering (SAXS) experiments were carried out using the SAXS instrument at the BL17B3 beamline of

the National Synchrotron Radiation Research Center (NSRRC), Taiwan. The blending samples of 1 mm thickness in general were sealed between two thin Kapton windows (80  $\mu\text{m}$  in thickness), and measured at room temperature.

## Results and Discussion

### The Synthesis of OT-POSS

In the hydrosilylated addition of  $\text{Q}_8\text{M}_8^{\text{H}}$  POSS with allyl-TEMPO, Karstedt's agent (a platinum divinylsiloxane complex) was used as a catalyst. For the reaction temperature at 50 °C for 4 h, the *N*-alkoxyamine groups are stable so as to chemically modify POSS cages. Monitoring the hydrosilylation by FTIR as shown in Figure 1 reveals that the hydrosilylation conversion increases up to 100% according to the silane stretching mode (Si–H, at 2134  $\text{cm}^{-1}$ ) after 4 h when the feeding molar ratio of  $\text{Q}_8\text{M}_8^{\text{H}}$  to allyl-TEMPO is 1:10. The quantitative hydrosilylation with 100% conversion plays an important role in the preparation of the well-defined POSS-based initiator. Figure 2 shows  $^1\text{H}$  NMR spectra of  $\text{Q}_8\text{M}_8^{\text{H}}$  POSS, OT-POSS, and allyl TEMPO. Clearly, the signals of the Si–H groups (4.7 ppm in Figure 2a) and vinyl protons (5.12 and 5.77 ppm in Figure 2c) in the reaction mixtures have disappeared in the spectrum of OT-POSS, which supports the complete reaction of hydrosilylation. The grafting degree of 7.97 on the purified OT-POSS cube determined from  $^1\text{H}$  NMR [signals (a + a') and j] matches well with the theoretically predicted octakis-functional chemical structure. The isomerism of hydrosilylation results in  $\beta$  [ $\text{RSiCH}_2\text{CH}_2\text{R}'$ ] and  $\alpha$  [ $\text{RSiCH}(\text{CH}_3)\text{R}'$ ] linkages, where R is the POSS core and R' is the organic functional group. The molar ratio of  $\beta$  to  $\alpha$  linkage is 1.11:1 according to the integration of the signals for  $-\text{CH}_2\text{O}-$  (signals f and f'). All FTIR and  $^1\text{H}$  NMR results indicate the successful synthesizing of OT-POSS.

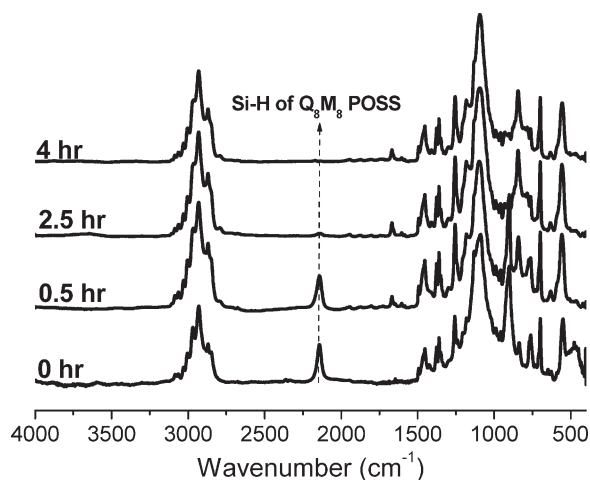


Figure 1. FTIR monitoring of hydrosilylation of OT-POSS.

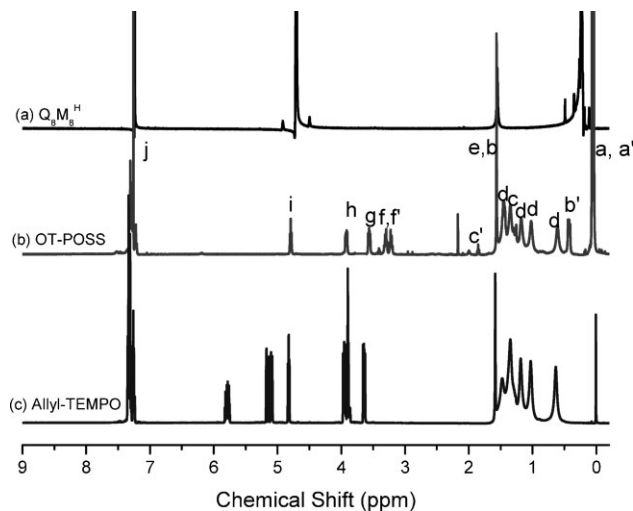


Figure 2.  $^1\text{H}$  NMR spectra of purified OT-POSS.

### The Synthesis of Star (PS)<sub>8</sub>-POSS Homopolymers

The synthesis of star polystyrene [(PS)<sub>8</sub>-POSS] from OT-POSS is the second step in the preparation of well-defined hybrid polymers using NMRP (Scheme 3). The NMRP polymerization without requiring metal catalyst and the initiation step from an unimolecular initiator are two major advantages over other living/controlled free radical polymerizations to simplify the purification and the polymerization.<sup>[36,42]</sup> In the NMRP of styrene, heating the mixture of OT-POSS ( $11.4 \times 10^{-3}$  M for target  $\bar{M}_n = 80\,000$  g  $\cdot$  mol $^{-1}$ ) and styrene at 120 °C gives monomer conversion at 80% after 17 h and star polystyrene with degree of polymerization ( $\bar{DP}_n$ ) = 77 for each arm based on the vinyl protons of styrene monomers (Figure 2b). In addition, Figure 3 shows the linear relationship between  $\ln(M_0/M)$  and reaction time indicates a first-order reaction for controllable polymerization. In comparison with styrene conversion

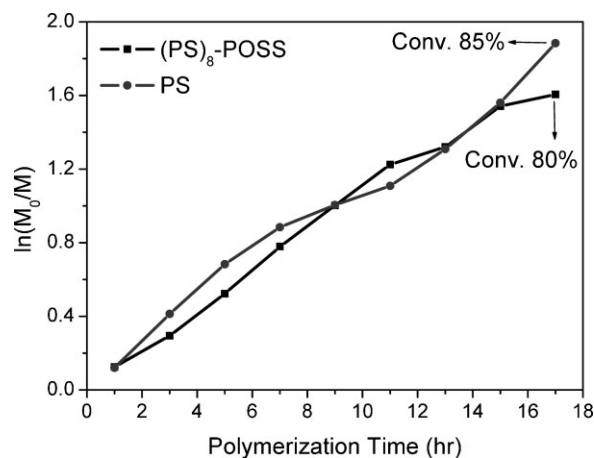


Figure 3. Conversion of linear PS and star (PS)<sub>8</sub>-POSS.

of 85% for linear polystyrene from the monofunctional *N*-alkoxyamine initiator ( $1.4 \times 10^{-3} \text{ M}$  for target  $\overline{M}_n = 10\,000 \text{ g} \cdot \text{mol}^{-1}$ ), the similar high conversions indicate that NMRP propagation from a POSS cube can suppress the steric effect of divergent polymerization for a star polymer, which would result in gelation at the relatively low conversion.<sup>[15]</sup> The theoretical molecular weight of  $67\,700 \text{ g} \cdot \text{mol}^{-1}$  for  $(\text{PS})_8\text{-POSS}$  was determined from  $^1\text{H}$  NMR ( $\overline{DP}_n$  theoretical = 77 for each arm at 17 h). In comparison with the results from  $^1\text{H}$  NMR and SEC, Figure 4 shows the shift of SEC distribution to high molar mass matches well with the increase of the monomer conversion. However, molecular weight determined from SEC is slightly lower than the theoretically predicted value ( $\overline{M}_n$  SEC =  $60\,600 \text{ g} \cdot \text{mol}^{-1}$  vs.  $\overline{M}_n$  theoretical  $67\,700$ ), and low polydispersities ( $\overline{M}_w/\overline{M}_n = 1.12$ ) are observed. The discrepancy between the observed SEC molecular weights and the theoretical values can be attributed to hydrodynamic difference between star PS sample and linear PS standards in DMF-*d*<sub>7</sub> mobile phase.

The large discrepancy of  $(\text{PS})_8\text{-POSS}$  between the SEC molecular weight and the  $^1\text{H}$  NMR-predicted value can be attributed to chemical confinement (smaller hydrodynamic volume) of eight PS chains onto a POSS cube. To clarify this discrepancy, the POSS cage was decomposed by the HF treatment.<sup>[32]</sup> Resultant mass distribution of the  $(\text{PS})_8\text{-POSS}$  after HF treatment became two narrower peaks (Figure 5a). In addition to the unreacted  $(\text{PS})_8\text{-POSS}$ , the new and lower molar-mass peak can be attributed to the PS arms ( $4\,200 \text{ g} \cdot \text{mol}^{-1}$ ), which is closed to the  $^1\text{H}$  NMR predicted value of  $4\,060 \text{ g} \cdot \text{mol}^{-1}$ . The FTIR spectra of  $(\text{PS})_8\text{-POSS}$  before and after HF treatment clearly show the decomposition of POSS cages based on the decreasing intensity of the Si–O–Si bond at  $1\,096 \text{ cm}^{-1}$  (Figure 5b).

In addition, Figure 6 shows the conventional second run DSC thermograms of  $(\text{PS})_8\text{-POSS}$  and after HF treatment of

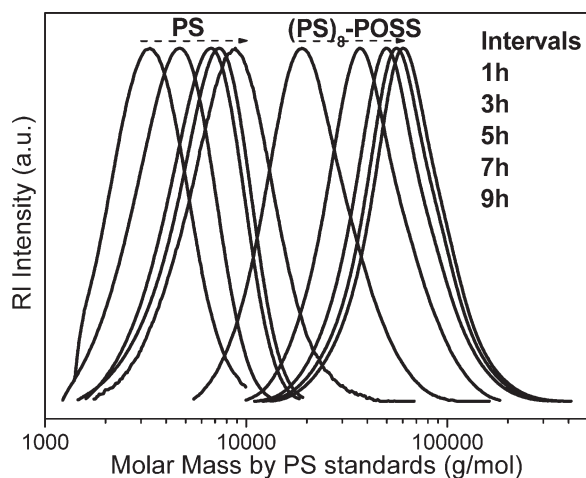


Figure 4. SEC trace of linear PS and star  $(\text{PS})_8\text{-POSS}$ .

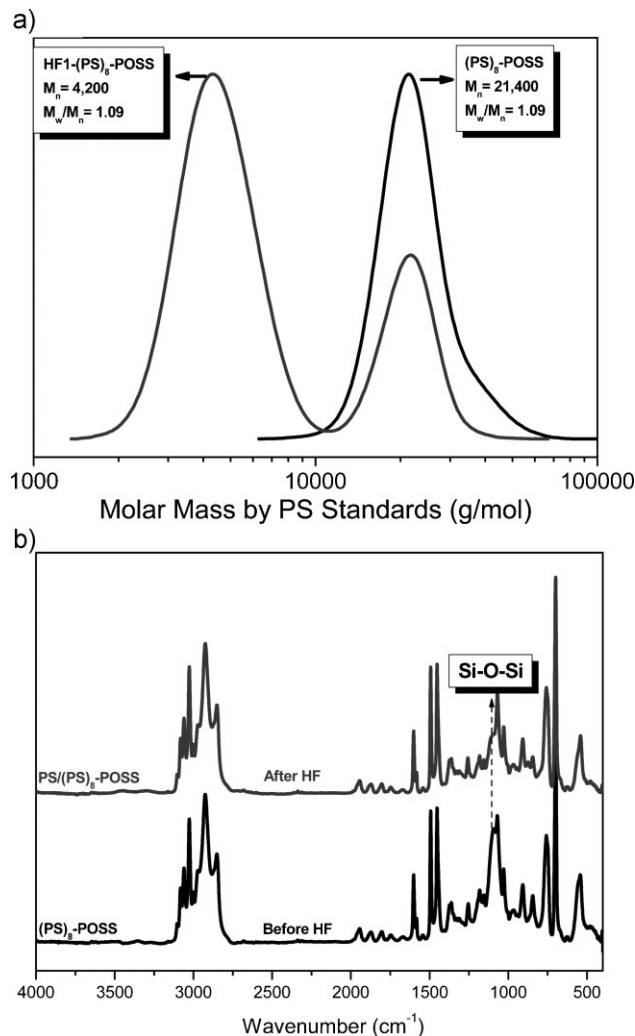


Figure 5. (a) SEC traces and (b) FTIR spectra of HF treatment of  $(\text{PS})_8\text{-POSS}$ .

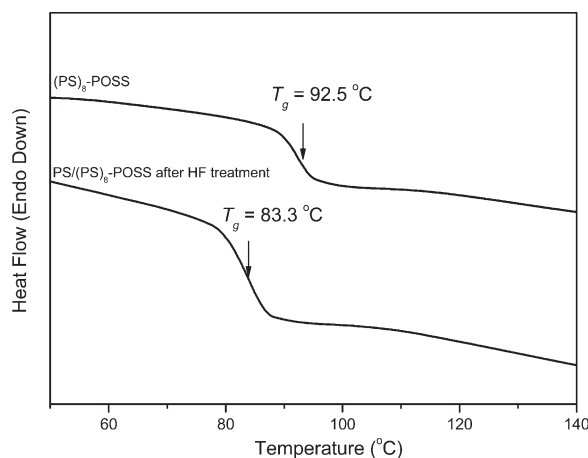


Figure 6. DSC of  $(\text{PS})_8\text{-POSS}$  and after HF treatment.

(PS)<sub>8</sub>-POSS. Glass transition temperature ( $T_g$ ) is one of the basic physical parameters of polymers. It was known that molecular weight (particularly at in the low range) and chain topology can considerably influence  $T_g$  value of a polymer. Moreover, it has been previously predicated and experimentally proven that star polymers generally possess slightly higher  $T_g$  value than their linear counterparts.<sup>[31]</sup> A comparison of DSC curve of star PS and linear PS after HF treatment, the linear PS were determined to 83.3 °C, which is lower than star PS (92.5 °C) since cleaving with HF results in the decrease of overall molecular weight and the increase of chain mobility by freeing of chain ends.

### The Synthesis of Star (PS-*b*-P4VP)<sub>8</sub>-POSS and (PS-*b*-PAS)<sub>8</sub>-POSS Block Copolymers

The synthesis of star block copolymer from (PS)<sub>8</sub>-POSS is the third step in the preparation of well-defined hybrid polymers using NMRP (Scheme 3). The pseudo-living NMRP polymerization can preserve the reactive chain ends containing *N*-alkoxyamine to incorporate other monomers. To obtain low molar mass of the (PS)<sub>8</sub>-POSS macroinitiator, the polymerization was paused at 5 h by quenching in the ice bath and the conversion of styrene monomers was around 41%. Analyses of the purified (PS)<sub>8</sub>-POSS by <sup>1</sup>H NMR revealed that the repeating units of PS per arm reached 39 (about 4 060 g · mol<sup>-1</sup>) based on the protons of -Si(CH<sub>3</sub>)<sub>3</sub> from the OT-POSS and that of PS phenyl ring (Figure 7b). Figure 8 shows the shift of SEC distribution from 21 400 g · mol<sup>-1</sup> (PS)<sub>8</sub>-POSS to 56 300 g · mol<sup>-1</sup> (PS-*b*-P4VP)<sub>8</sub>-POSS or 53 900 g · mol<sup>-1</sup> (PS-*b*-PAS)<sub>8</sub>-POSS demonstrated the versatility of “living” free radical polymerizations of second monomers such as 4-vinylpyridine and 4-acetoxystyrene from the (PS)<sub>8</sub>-POSS macroinitiator.

Figure 7a presents the FTIR spectra of (PS)<sub>8</sub>-POSS, (PS-*b*-P4VP)<sub>8</sub>-POSS, and (PS-*b*-PAS)<sub>8</sub>-POSS. Two peaks were present for the pyridine groups (strong absorption at 1 596 cm<sup>-1</sup> and weak absorption at 993 cm<sup>-1</sup>) providing evidence for the 4-vinylpyridine unit in (PS-*b*-P4VP)<sub>8</sub>-POSS. In addition, a strong peak was observed for the C=O groups from the acetoxystyrene units (1 765 cm<sup>-1</sup>), of (PS-*b*-PAS)<sub>8</sub>-POSS also providing evidence for the successful attachment of the acetoxystyrene units to the (PS)<sub>8</sub>-POSS core. Figure 7b shows their corresponding <sup>1</sup>H NMR spectra of (PS)<sub>8</sub>-POSS, (PS-*b*-PAS)<sub>8</sub>-POSS, and (PS-*b*-P4VP)<sub>8</sub>-POSS. Analyses of the purified (PS-*b*-PAS)<sub>8</sub>-POSS and (PS-*b*-P4VP)<sub>8</sub>-POSS by <sup>1</sup>H NMR revealed that the repeating units of P4VP and PAS per arm reached 20 (about 2 100 g · mol<sup>-1</sup>) and 24 (about 3 890 g · mol<sup>-1</sup>) by comparing protons from the styryl (7.07 ppm), pyridyl (8.34 ppm), and methyl (2.27 ppm) protons.

Figure 9 shows the conventional second run DSC thermograms of (PS)<sub>8</sub>-POSS, (PS-*b*-PAS)<sub>8</sub>-POSS, and (PS-*b*-P4VP)<sub>8</sub>-POSS. Clearly, both (PS-*b*-PAS)<sub>8</sub>-POSS ( $T_g$  = 101.1 and

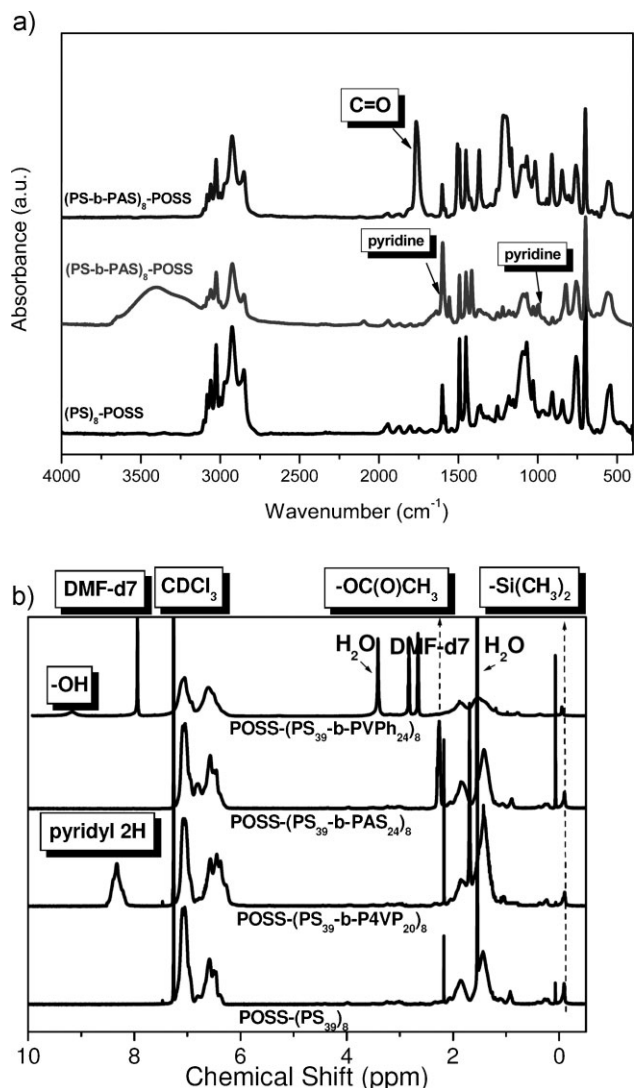


Figure 7. (a) FTIR of star block (PS)<sub>8</sub>-POSS, (PS-*b*-P4VP)<sub>8</sub>-POSS, and (PS-*b*-PAS)<sub>8</sub>-POSS and (b) <sup>1</sup>H NMR spectra of star block (PS)<sub>8</sub>-POSS, (PS-*b*-P4VP)<sub>8</sub>-POSS, (PS-*b*-PAS)<sub>8</sub>-POSS, and ((PS-*b*-PVPh)<sub>8</sub>-POSS.

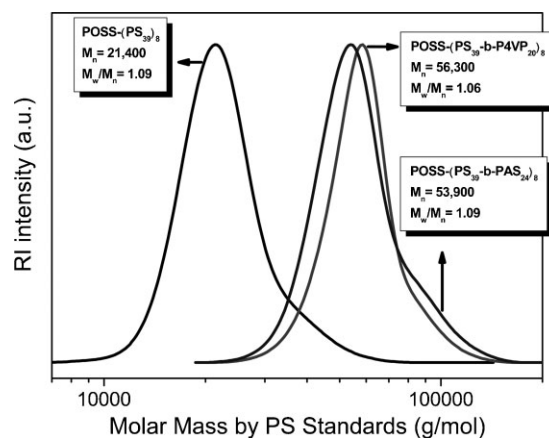


Figure 8. SEC trace of star block (PS)<sub>8</sub>-POSS, (PS-*b*-P4VP)<sub>8</sub>-POSS, and (PS-*b*-PAS)<sub>8</sub>-POSS.

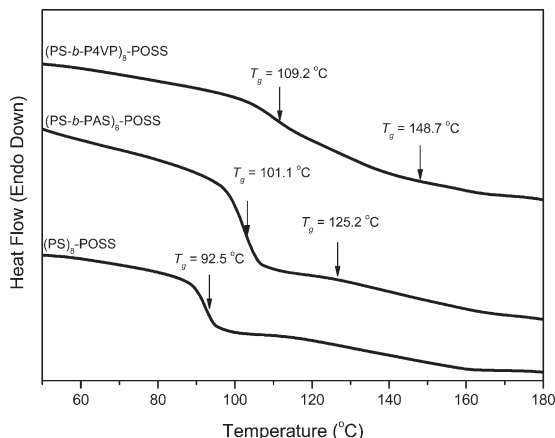


Figure 9. DSC thermograms of  $(PS)_8$ -POSS,  $(PS-b-PAS)_8$ -POSS, and  $(PS-b-P4VP)_8$ -POSS.

125.2 °C) and  $(PS-b-P4VP)_8$ -POSS ( $T_g = 109.2$  and 148.7 °C) exhibit two glass transitions, indicating that chemical incompatibility between the constituent blocks leads to phase separation. The lower  $T_g$  is corresponding to PS block and higher  $T_g$  is corresponding to PAS or P4VP block segments, respectively. In addition, the value of  $T_g$  of the PS block in diblock copolymers was higher than that of PS homopolymer, presumably because of hard confinement and the presence of fewer chain ends.<sup>[43–45]</sup> The PS block segment in diblock copolymer maybe exist in the form of a more-compact packing order nanostructure, resulting in smaller free volume and higher value of  $T_g$ . The self-assembly structure of  $(PS-b-P4VP)_8$ -POSS diblock copolymer could be characterized by TEM and SAXS analyses as shown in Figure 10.  $(PS-b-P4VP)_8$ -POSS diblock copolymer exhibits

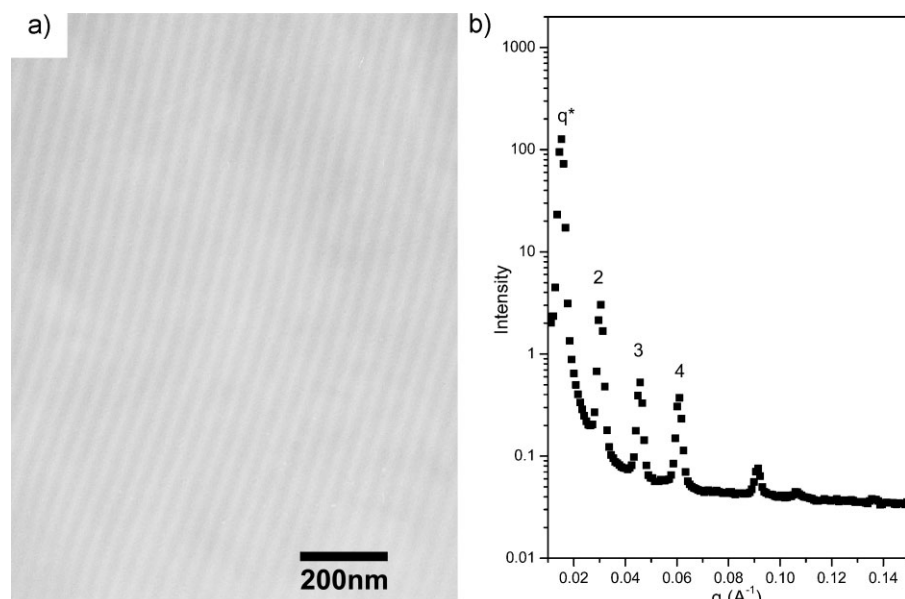


Figure 10. Self-assembly structure of  $(PS-b-P4VP)_8$ -POSS: (a) TEM image and (b) SAXS analysis.

an alternating lamellar morphology and long-range order pattern with lamellar period of ca. 40 nm as shown in TEM image (Figure 10a), which is consistent with SAXS analysis in Figure 10b. The SAXS analysis has a lamellar microdomain structure, judging from the scattering maxima at relative positions of 1:2:3:4. Couple SAXS peaks located at the positions of multiple  $Q_c = 0.01517 \text{ \AA}^{-1}$  indicates a lamellar phase with a long period of 40.5 nm extracted from the first peak position ( $2\pi/Q_c$ ).

### The Synthesis of Star $(PS-b-PVPh)_8$ -POSS Block Copolymers

Subsequent deprotection of the acetoxy groups of the PAS block with hydrazine monohydrate led to the  $(PS-b-PVPh)_8$ -POSS star block copolymer. The mass distribution of  $(PS-b-PAS)_8$ -POSS after  $N_2H_4$  treatment became another new peak as shown in Figure 7b and Figure 11a. This broader molar-mass distribution can be attributed to the chromatographic tailing from the hydrogen bonding of eight PVPh arms. In Figure 7b, a chemical shift at 2.2 ppm corresponds to the acetyl group of the  $(PS-b-PAS)_8$ -POSS (in  $DMSO-d_6$ ). These peaks corresponding to the acetyl group are essentially disappeared from the spectrum of the hydrolyzed block copolymer only these polymer backbone protons appear in the chemical shift region of 1–2 ppm. In addition, a peak (9.0 ppm) corresponding to the proton of the hydroxyl group appears after hydrolysis reaction. FTIR spectra of  $(PS-b-PAS)_8$ -POSS before and after  $N_2H_4$  treatment can apparently indicate the deprotection of acetoxy groups at  $1760 \text{ cm}^{-1}$  and the formation of phenols at  $3350 \text{ cm}^{-1}$  corresponding

to multiple hydrogen bonding of hydroxyl–hydroxyl in PVPh block as shown in Figure 11b.

Figure 12 shows the conventional second run DSC thermograms of  $(PS-b-PAS)_8$ -POSS, and  $(PS-b-PVPh)_8$ -POSS. Clearly, the  $T_g$  value of PAS block (125.2 °C) shifts to 182.3 °C of PVPh block in POSS diblock copolymers due to the strong hydroxyl–hydroxyl hydrogen bonding interaction in PVPh block segment that would decrease the free volume of chain segment.<sup>[46,47]</sup> In addition, the value of  $T_g$  of the PS block in diblock copolymers in  $(PS-b-PVPh)_8$ -POSS was higher than that in  $(PS-b-PAS)_8$ -POSS presumably due to the PS block connected different polymer segments since stronger hard confinement

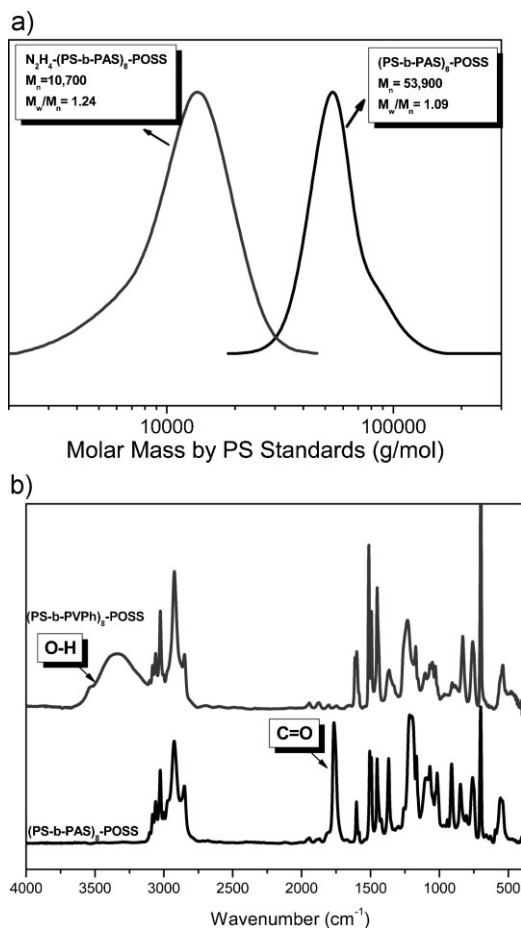


Figure 11. (a) SEC traces and (b) FTIR spectra of (PS-*b*-PAS)<sub>8</sub>-POSS after N<sub>2</sub>H<sub>4</sub> hydrolysis reaction ((PS-*b*-PVPh)<sub>8</sub>-POSS).

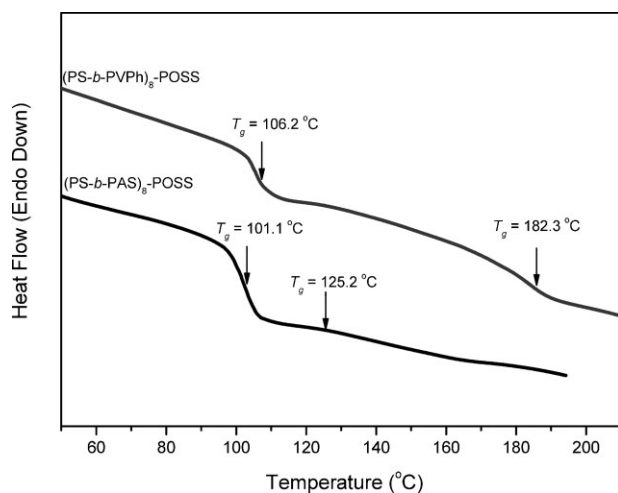


Figure 12. DSC thermograms of (PS-*b*-PAS)<sub>8</sub>-POSS and (PS-*b*-PVPh)<sub>8</sub>-POSS.

of PVPh ( $T_g = 182.3^\circ\text{C}$ ) than PAS ( $T_g = 125.2^\circ\text{C}$ ). In addition, (PS-*b*-PVPh)<sub>8</sub>-POSS containing a strongly hydrogen-donating poly(vinyl phenol) block onto a relatively hydrophobic polystyrene core. In contrast, star block (PS-*b*-P4VP)<sub>8</sub>-POSS possess a strongly hydrogen-accepting poly(4-vinylpyridine) block is attached to a relatively hydrophobic polystyrene core. The hydrogen bonding blends of star block copolymers appeal our interest in the further study.

## Conclusion

We have synthesized novel hybrid polymers from a POSS-based initiator using NMRP. From this approach, star homopolymer and block copolymers have been prepared such as PS homopolymer, PS-*b*-P4VP, PS-*b*-PAS, and PS-*b*-PVPh diblock copolymers. The characteristic of living free radical polymerization from a POSS-based initiator or macroinitiator was investigated by <sup>1</sup>H NMR and FTIR spectra and SEC analyses. The detailed self-assembly structure of these star block copolymers based on POSS were characterized by DSC, TEM, and SAXS analyses. TEM imaging and SAXS indicate that long-range order of lamellae of (PS-*b*-P4VP)<sub>8</sub>-POSS diblock copolymer and the self-assembly behavior of hydrogen bonding blends of star (PS-*b*-PVPh)<sub>8</sub>-POSS with (PS-*b*-P4VP)<sub>8</sub>-POSS diblock copolymer mixture will be further studied in the near future.

**Acknowledgements:** This study was supported financially by the National Science Council, Taiwan, Republic of China, under Contract Nos. NSC 97-2221-E-110-013-MY3 and NSC 97-2120-M-009-003.

Received: January 26, 2010; Published online: March 18, 2010;  
DOI: 10.1002/macp.201000051

**Keywords:** block copolymers; hydrogen bonding; POSS; self-assembly; star polymers

- [1] J. A. Simms, H. J. Spinelli, "Macromolecular Design of Polymeric Materials", K. Hatada, T. Kitayama, O. Vogl, Eds., Marcel Dekker, New York 1997.
- [2] S. Bywater, *Adv. Polym. Sci.* **1979**, *30*, 90.
- [3] T. M. Marsalko, I. Majoros, J. P. Kennedy, *Pure Appl. Chem.* **1997**, *34*, 775.
- [4] M. Morton, T. E. Helminiak, S. D. Gadkary, F. Bueche, *J. Polym. Sci.* **1962**, *57*, 471.
- [5] A. W. Bosman, A. Heumann, G. Klaerner, D. Benoit, J. M. J. Frechet, C. J. Hawker, *J. Am. Chem. Soc.* **2001**, *123*, 6461.
- [6] K. Matyjaszewski, P. J. Miller, J. Pyun, G. Kickelbick, S. Diamanti, *Macromolecules* **1999**, *32*, 6526.
- [7] D. Yan, Z. Zhou, *Macromolecules* **1999**, *32*, 245.
- [8] G. I. Litvinenko, A. H. E. Müller, *Macromolecules* **2002**, *35*, 4577.



- [9] H. Hussain, B. H. Tan, C. S. Gudipati, Y. Xiaio, Y. Liu, T. P. Davis, C. B. He, *J. Polym. Sci., Part A: Polym. Chem.* **2008**, *46*, 7287.
- [10] M. Sawamoto, "Cationic Polymerizations", K. Matyjaszewski, Ed., Marcel Dekker, New York 1996.
- [11] J. P. Kennedy, S. Jacob, *Acc. Chem. Res.* **1998**, *31*, 835.
- [12] E. Cloutet, J. Fillaut, D. Astruc, Y. Gnanou, *Macromolecules* **1998**, *31*, 6748.
- [13] R. Quirk, Y. Tsai, *Macromolecules* **1998**, *31*, 8016.
- [14] C. F. Huang, H. F. Lee, S. W. Kuo, H. Xu, F. C. Chang, *Polymer* **2004**, *45*, 2261.
- [15] S. C. Chan, S. W. Kuo, F. C. Chang, *Macromolecules* **2005**, *38*, 3099.
- [16] K. Inoue, *Prog. Polym. Sci.* **2000**, *25*, 453.
- [17] H. Xu, S. W. Kuo, J. S. Lee, F. C. Chang, *Macromolecules* **2002**, *35*, 8788.
- [18] G. Z. Li, L. C. Wang, H. L. Ni, C. U. Pittman, *J. Inorg. Organomet. Polym.* **2001**, *11*, 123.
- [19] S. H. Phillips, T. S. Haddad, S. J. Tomczak, *Curr. Opin. Solid State Mater. Sci.* **2004**, *8*, 21.
- [20] M. Joshi, B. S. Butola, *J. Macromol. Sci. Polym. Rev.* **2004**, *C44*, 389.
- [21] J. E. Mark, *Acc. Chem. Res.* **2004**, *37*, 946.
- [22] K. Pielichowski, J. Niuguna, B. Janwski, B. Pielichowski, *Adv. Polym. Sci.* **2006**, *201*, 225.
- [23] P. D. Lickiss, F. Rataboul, *Adv. Organomet. Chem.* **2008**, *57*, 1.
- [24] J. Choi, J. Harcup, A. F. Yee, Q. Zhu, R. M. Laine, *J. Am. Chem. Soc.* **2001**, *123*, 11420.
- [25] R. Tamaki, Y. Tanaka, M. Z. Asuncion, J. Choi, R. M. Laine, *J. Am. Chem. Soc.* **2001**, *123*, 12416.
- [26] C. F. Huang, S. W. Kuo, F. J. Lin, W. J. Huang, C. F. Wang, W. Y. Chen, F. C. Chang, *Macromolecules* **2006**, *39*, 300.
- [27] H. C. Lin, S. W. Kuo, C. F. Huang, F. C. Chang, *Macromol. Rapid Commun.* **2006**, *27*, 537.
- [28] S. C. Chan, S. W. Kuo, H. S. She, H. F. Lee, F. C. Chang, *J. Polym. Sci.: Polym. Chem. Ed.* **2007**, *45*, 125.
- [29] S. W. Kuo, H. F. Lee, W. J. Huang, K. U. Jeong, F. C. Chang, *Macromolecules* **2009**, *42*, 1619.
- [30] C. H. Lu, S. W. Kuo, C. F. Huang, F. C. Chang, *J. Phys. Chem. C* **2009**, *113*, 3517.
- [31] Z. Ge, D. Wang, Y. Zhou, H. Liu, S. Y. Liu, *Macromolecules* **2009**, *42*, 2903.
- [32] R. O. R. Costa, W. L. Vasconcelos, R. Tamaki, R. M. Laine, *Macromolecules* **2001**, *34*, 5398.
- [33] S. C. Chan, S. W. Kuo, C. H. Lu, H. F. Lee, F. C. Chang, *Polymer* **2007**, *48*, 5059.
- [34] C. H. Lu, C. F. Huang, S. W. Kuo, F. C. Chang, *Macromolecules* **2009**, *42*, 1067.
- [35] W. C. Chen, S. W. Kuo, C. H. Lu, F. C. Chang, *Macromolecules* **2009**, *42*, 3580.
- [36] C. J. Hawker, A. W. Bosman, E. Harth, *Chem. Rev.* **2001**, *101*, 3661.
- [37] I. H. Lin, S. W. Kuo, F. C. Chang, *Polymer* **2009**, *50*, 5276.
- [38] S. C. Chen, S. W. Kuo, U. S. Jeng, F. C. Chang, *Macromolecules* **2010**, *43*, 1083.
- [39] S. W. Kuo, C. F. Huang, C. H. Lu, H. M. Lin, K. U. Jeong, F. C. Chang, *Macromol. Chem. Phys.* **2006**, *207*, 2006.
- [40] Y. C. Sheen, C. H. Lu, C. F. Huang, S. W. Kuo, F. C. Chang, *Polymer* **2008**, *49*, 4017.
- [41] K. W. Huang, L. W. Tsai, S. W. Kuo, *Polymer* **2009**, *50*, 4876.
- [42] V. Sciannamea, R. Jerome, C. Detrembleur, *Chem. Rev.* **2008**, *108*, 1104.
- [43] U. Gaur, B. Wunderlich, *Macromolecules* **1980**, *13*, 1618.
- [44] J. Bares, *Macromolecules* **1975**, *8*, 244.
- [45] J. Q. Zhao, E. M. Pearce, T. K. Kwei, *Macromolecules* **1997**, *30*, 7119.
- [46] S. W. Kuo, F. C. Chang, *Polymer* **2003**, *44*, 3021.
- [47] S. W. Kuo, H. Y. Xu, C. F. Huang, F. C. Chang, *J. Polym. Sci.: Polym. Phys.* **2002**, *40*, 2313.